Electroreduction of Carbon Dioxide by Homogeneous Iridium Catalysts

Ryoichi Kanega

Contents

Abstract The electroreduction of carbon dioxide (CO_2) to chemical fuels provides not only a means to utilize CO_2 but also a solution to challenges relating to the storage and transport of renewable energy. For this purpose, a range of catalysts for the electroreduction of CO_2 have been studied, and recent progress in the context of tuning catalytic properties and understanding their mechanism of action has been remarkable. For example, molecular approaches allow fine-tuning of the catalyst behavior by the design of suitable ligands to suppress the overpotential for CO_2 conversion. This chapter focuses on homogeneous iridium catalysts for the electroreduction of CO_2, whereby the examples provided give mechanistic insight into the design of catalysts to efficiently and selectively produce electroreduced compounds from CO_2 using electricity.

R. Kanega (✉)
Research Institute of Energy Conservation, National Institute of Advanced Industrial Science and Technology, Tsukuba, Ibaraki, Japan
e-mail: r-kanega@aist.go.jp

1 Introduction

To reduce the carbon dioxide (CO_2) emissions associated with the consumption of fossil fuels [1], it is necessary to utilize various technologies, such as renewable energy and energy-saving technologies. Recently, the price of renewable energy has drastically decreased, and so its usage is expected to increase [2]. However, the lack of established methods for the storage and transport of electricity derived from renewable energy sources remains a challenge that hinders its use. For example, the storage and transportation of electricity is essential if the electricity generated during the day is to be used at night, or in places without a power grid. In this context, chemical fuels produced electrochemically have the potential to address these issues compared to other methods, such as chemical and photochemical reactions [3, 4]. In particular, one attractive approach involves the use of electricity derived from renewable energy sources to produce chemical fuels from CO_2 and H_2O (an H^+ source) [5].

The redox potentials of typical chemical fuels obtained by the electroreduction of CO_2 are shown in Table 1 [6–8]. Generally, in the electroreduction of CO_2, proton-coupled multi-electron transfer is more favorable than multi-electron transfer, as thermodynamically more stable compounds are produced. The single-electron transfer of CO_2 to $CO_2^{\cdot-}$ requires a large redox potential of -1.90 V (vs the standard hydrogen electrode (SHE); all potentials are given with respect to this reference), a large reorganization energy between the linear molecule and bent radical anion [9]. On the other hand, proton-coupled multi-electron transfer is achieved using a potential lower than -1.0 V. However, the development of efficient catalysts is necessary to carry out the intended electrochemical transformations with low overpotentials and high current densities.

To date, significant efforts have been devoted to the exploration of potential homogeneous and heterogeneous catalysts. For example, heterogeneous catalysts based on various metals, such as copper, cobalt, and tin, have been reported [10];

Table 1 Selected redox potentials for the electroreduction of CO_2 and generation of hydrogen (vs SHE in aqueous solution at pH 7)

Product	n^a	Cathode reaction	E^0 [V]
CO	2	$CO_2 + 2H^+ + 2e^- \rightarrow CO + H_2O$	-0.53
HCO_2^-	2	$CO_2 + H^+ + 2e^- \rightarrow HCO_2^-$	-0.49
HCO_2H	2	$CO_2 + 2H^+ + 2e^- \rightarrow HCO_2H$	-0.61
CH_3OH	6	$CO_2 + 6H^+ + 6e^- \rightarrow CH_3OH + H_2O$	-0.38
CH_4	8	$CO_2 + 8H^+ + 8e^- \rightarrow CH_4 + 2H_2O$	-0.24
$C_2O_4^{2-}$	2	$2CO_2 + 2e^- \rightarrow C_2O_4^{2-}$	-1.00
$CO_2^{\cdot-}$	1	$CO_2 + e^- \rightarrow CO_2^{\cdot-}$	-1.90
H_2	2	$2H^+ + 2e^- \rightarrow H_2$	-0.41

$^a n$ Number of reaction electrons

however, in many cases, the conversion of CO_2 involves inefficient $CO_2^{\cdot-}$ formation. On the other hand, homogeneous catalysts, such as ruthenium-, rhodium-, and iridium-based complexes, often form metal hydrides as intermediates [11, 12]. This circumvents the $CO_2^{\cdot-}$ formation, and hence, more efficient electrochemical conversions are expected. For example, $[Rh(bpy_2(TFMS)_2)]^+$ (bpy, 2,2′-bipyridine; TFMS, trifluoromethanesulfonate anion) exhibited 80% Faradaic efficiency (FE) for HCO_2^- production in CH_3CN at -0.96 V. Moreover, electroreduction of CO_2 in aqueous solution was achieved with high FE at a very low overpotential using iridium catalysts. This chapter, therefore, describes the development of iridium-based homogeneous catalysts for the electroreduction of CO_2 to formate (HCO_2^-), carbon monoxide (CO), and oxalate ($C_2O_4^{2-}$).

2 Electroreduction of Carbon Dioxide to Formate

2.1 Homogeneous Catalysts

HCO_2^- (HCO_2H), a two-electron reduction product of CO_2, has recently attracted significant attention as a liquid organic hydrogen (H_2) carrier, in which H_2 is established as a new energy vector [13, 14]. Through HCO_2^- (HCO_2H) dehydrogenation (Eqs. 1 and 2), H_2 can be released with a lower energy consumption than those required for other H_2 storage media, such as methylcyclohexane or ammonia. Furthermore, in contrast to other chemical H_2 carriers, HCO_2H can produce high-pressure H_2 using only thermal reactions [15]. The potential for the CO_2 to HCO_2^- transformation is -0.49 V, which indicates a slightly higher energy consumption than H_2 generation (-0.41 V). If the electroreduction of CO_2 to HCO_2^- can be realized with a high FE (Eq. 3, where X is a product such as CO, HCO_2^-, $C_2O_4^{2-}$ or H_2, F is the Faraday constant, and n is the number of reaction electrons) and a low overpotential, it becomes an energy storage method comparable to water electrolysis. Additionally, C-H bond formation is one of the most essential elementary reactions in synthetic chemistry. The conversion of CO_2 to HCO_2^- (HCO_2H) involves C-H bond formation, which can be considered as an electrochemical method of C-H bond formation.

$$HCO_2^- + H_2O \rightarrow H_2 + CO_2 + OH^- \tag{1}$$

$$HCO_2H \rightarrow H_2 + CO_2 \tag{2}$$
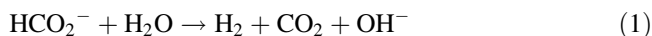
$$FE(X)\ [\%] = F\ [C\ mol^{-1}] \times n\ X\ [mol]/total\ Q\ [C] \times 100 \tag{3}$$

In 1996, $[Ir_2(dimen)_4]^{2+}$ (dimen, 1,8-diisocyano-n-menthane) was studied using infrared spectro-electrochemistry, whereby HCO_2^- and bicarbonate were detected, although the products were not quantified [16]. In addition, the obtained results indicated that $[Ir_2(dimen)_4]^{2+}$ accepted 2 electrons to form $[Ir_2(dimen)_4]^0$, which then reacted with CO_2 and H_2O. In addition, the electroreduction of CO_2 to HCO_2^- was reported using $[Cp^*Ir(bpy)Cl]^+$ (Cp^*, pentamethylcyclopentadienyl) in CH_3CN

Chart 1 Catalysts for the electroreduction of CO_2 to HCO_2^-

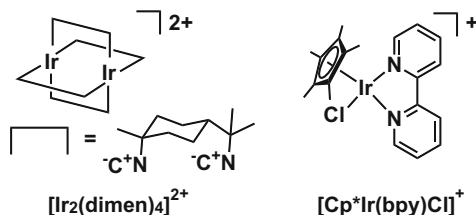$[Ir_2(dimen)_4]^{2+}$ $[Cp*Ir(bpy)Cl]^+$

Table 2 Electroreduction of CO_2 to HCO_2^-

Catalyst	Solvent	E_{app}[a] [V]	FE(HCO_2^-) [%]	j [mA cm^{-2}]	Ref.
$[Ir_2(dimen)_4]^{2+}$	THF/H_2O	−1.62	–	–	[16]
$[Cp*Ir(bpy)Cl]^+$	CH_3CN	−1.16	22	132	[17]

[a]E_{app} Applied potential

(POCOP)IrH$_2$ [(POCOP')Ir(sol)$_2$H]$^{2+}$
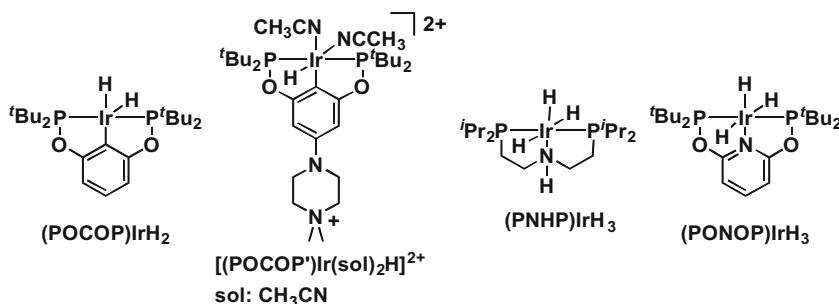sol: CH$_3$CN   (PNHP)IrH$_3$ (PONOP)IrH$_3$

Chart 2 Catalysts bearing pincer ligands for the electroreduction of CO_2 to HCO_2^-

(Chart 1, Table 2) [17]. Electrolysis was performed at −1.16 V, and HCO_2^- was produced with an FE(HCO_2^-) of 22% (132 mA cm^{-2}). Although the formation of CO (FE(CO) < 1%) was confirmed, no other products were identified. Furthermore, based on the hydrogenation of CO_2, the electroreduction mechanism was speculated to involve reaction between the iridium-hydride intermediates and CO_2.

The reactivities and properties of a range of iridium-hydride species have been studied actively. Among them, iridium catalysts bearing a pincer ligand were found to exhibit a high activity and durability for the hydrogenation of CO_2 [18, 19]. In addition, through the use of related pincer ligands, electrochemically formed iridium-hydride species were investigated for the electroreduction of CO_2 (Chart 2, Table 3). For example, the potentiostatic electrolysis of (POCOP)IrH$_2$ was carried out at −1.45 V in a CH$_3$CN/5% H_2O solution to yield HCO_2^- in an FE(HCO_2^-) of 85% (1.07 mA cm^{-2}), whereby H_2 was detected as a by-product (FE(H_2) 15%) [20]. Moreover, through the introduction of 1,1-dimethyl-piperazinium to the pincer ligand, the FE(HCO_2^-) reached 93% in a water-based electrolyte (NaHCO$_3$/1% CH$_3$CN) [21]. Although CH$_3$CN was essential in the desorption of HCO_2^- from the iridium species and thus to promote catalyst turnover, [(POCOP')Ir(sol)$_2$H]$^{2+}$ (sol,

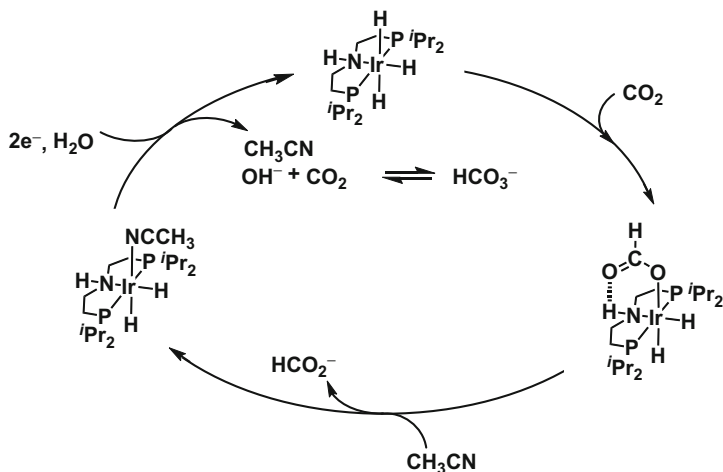**Table 3** Electroreduction of CO_2 to HCO_2^- using iridium complexes bearing pincer ligands

Catalyst	Solvent	E_{app}[a] [V]	FE(HCO_2^-) [%]	j [mA cm^{-2}]	Ref.
(POCOP)IrH$_2$	CH$_3$CN/5% H$_2$O	−1.45	85	1.07	[20]
[(POCOP′)IrH(sol)$_2$]$^{2+}$	NaHCO$_3$/1% CH$_3$CN	−1.41	93	0.60	[21]
(PNHP)IrH$_3$	CH$_3$CN/12% H$_2$O	−0.81	97	0.45	[22]
(PONOP)IrH$_3$	CH$_3$CN/5% H$_2$O	−1.15	97	2.10	[23]

[a]E_{app} Applied potential
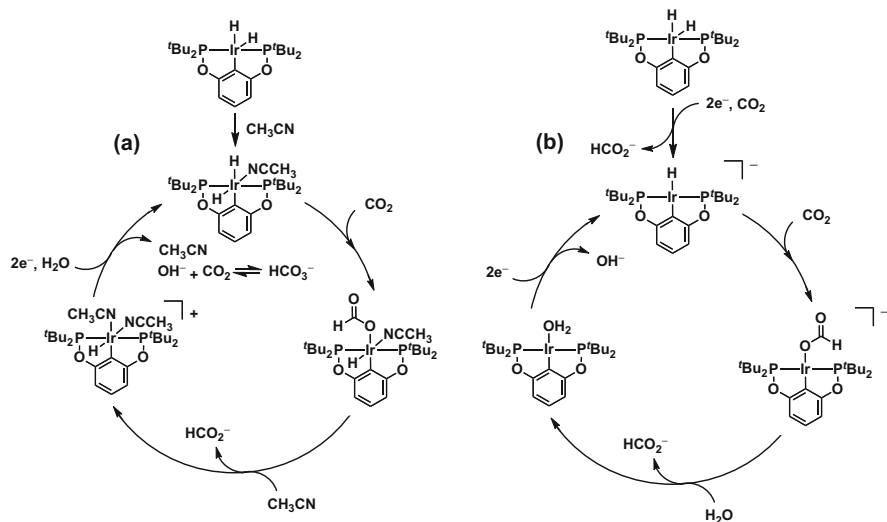
Scheme 1 Proposed mechanisms for the electroreduction of CO_2 with (**a**) (POCOP)IrH$_2$ by iridium(III) dihydride and (**b**) (POCOP)IrH$_2$ iridium(I) monohydride

CH$_3$CN) was also active, even in aqueous solution with a small amount of organic additive.

Subsequently, DFT calculations were employed to examine the reaction mechanism of the (POCOP)IrH$_2$ catalytic system [24]. As indicated in Scheme 1a, it was suggested that the reaction proceeds in three steps: (1) insertion of CO_2 into the iridium-hydride complex, (2) elimination of HCO_2^- from the resulting hydride-formate-iridium complex, and (3) regeneration of the active species. The reduction potential of the electrode reaction was calculated and was found to correspond with the experimental value. The solvents were also examined, and it was found that water was necessary for the transformation of CO_2 to HCO_2^-. Moreover, DFT calculations showed that HCO_2^- formation also involved iridium(I) monohydride as an active species formed in situ (Scheme 1b) [25]. It should be noted that the iridium(III) path can operate in parallel, but is associated with higher Gibbs free energies in the reaction between the iridium(III) dihydride species and CO_2 (i.e.,

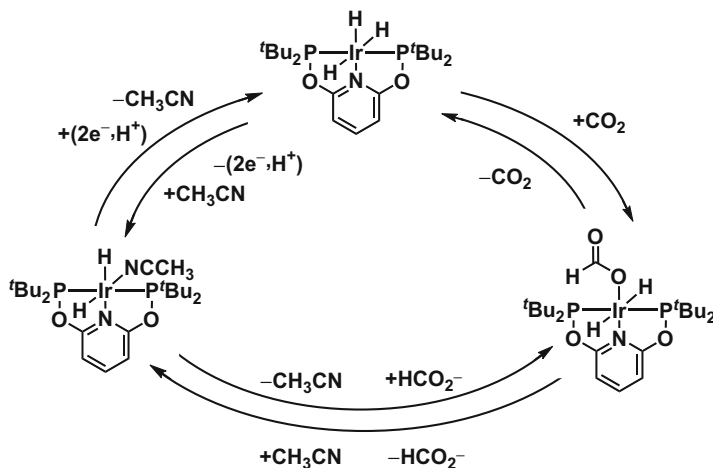**Scheme 2** Proposed mechanism for the electroreduction of CO_2 using $(PNHP)IrH_3$

16.6 and 19.0 kcal mol^{-1}), compared to the reaction between the in situ formed iridium(I) monohydride species (i.e., 12.3 kcal mol^{-1}).

An iridium trihydride complex bearing a PNHP ligand with a secondary coordination sphere interactions was found to improve the catalytic activity in CH_3CN/ 12% H_2O solution [22]. At -0.81 V, $(PNHP)IrH_3$ yielded HCO_2^- with an FE (HCO_2^-) of 97% (0.45 mA cm^{-2}). Mechanistic studies indicated that the insertion of CO_2 was accelerated by the presence of an NH group, and this was followed by HCO_2^- elimination and catalyst regeneration through an electroreduction/proton transfer mechanism (Scheme 2). Furthermore, the kinetic studies of $(PNHP)IrH_3$ appeared that the rate-determining step was HCO_2^- elimination, which can be enhanced by the addition of stabilizing agents such as water and Lewis acid.

Furthermore, an iridium trihydride complex bearing a PONOP pincer ligand was found to function not only in the electroreduction of CO_2 to HCO_2^- but also in the electrooxidation of HCO_2^- to CO_2 (Eq. 4) [23].

$$HCO_2^- \rightarrow CO_2 + H^+ + 2e^- \tag{4}$$
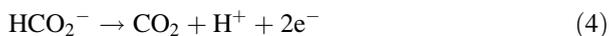
When the electroreduction of CO_2 in CH_3CN/5% H_2O was conducted at -1.15 V using $(PONOP)IrH_3$, the FE(HCO_2^-) reached 97% (2.1 mA cm^{-2}). In addition, HCO_2^- electrooxidation was carried out at 0.1 V in CH_3CN in the presence of $NBu_4HCO_2 \cdot HCO_2H$, whereby CO_2 was detected as the sole product. Quantification of the evolved CO_2 indicated an FE(CO_2) 88%. Electrochemical and NMR spectroscopic studies suggested that the hydride species is critical for the bifunctional reactivity. A potential catalytic mechanism for the reaction involving (PONOP) IrH_3 is outlined in Scheme 3. More specifically, CO_2 was inserted into (PONOP) IrH_3 to yield a HCO_2^- complex $(PONOP)IrH_2(HCO_2^-)$, which released HCO_2^- to give $(PONOP)Ir(CH_3CN)H_2$. Subsequent reduction yielded $(PONOP)IrH_3$. The

Scheme 3 Proposed mechanism for the electroreduction of CO_2 and the electrooxidation of HCO_2^- with $(PONOP)IrH_3$
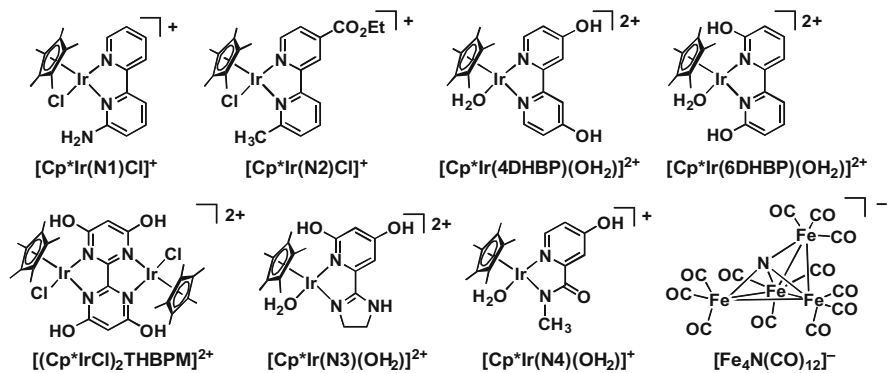

Chart 3 Catalysts bearing *N,N*-bidentate ligands and Fe carbonyl clusters for the electroreduction of CO_2 to HCO_2^-

HCO_2^- electrooxidation pathway is also illustrated in Scheme 3. More specifically, $(PONOP)IrH_3$ was oxidized electrochemically to form $(PONOP)Ir(CH_3CN)H_2$. In an equilibrium, $(PONOP)Ir(CH_3CN)H_2$ reacts rapidly with HCO_2^- to generate $(PONOP)IrH_2(HCO_2^-)$, and this was followed by β-hydride elimination to generate $(PONOP)IrH_3$ and CO_2. The applicability of this homogeneous catalyst in both the electroreduction and electrooxidation steps is interesting due to such a system only having been reported once previously (i.e., $[Pt(depe)_2]^{2+}$; depe, 1,2-bis(diethyl-phosphino)ethane) [26].

In addition to pincer ligands, catalysts based on iridium-hydride species bearing *N, N*-bidentate ligands have also been developed (Chart 3). The influence of

Table 4 Electroreduction of CO_2 to HCO_2^- using iridium complexes bearing *N,N*-bidentate ligands

Catalyst	Solvent	E_{app}[a] [V]	FE(HCO_2^-) [%]	j [mA cm^{-2}]	Ref.
[Cp*Ir(**N1**)cl]$^+$	CH$_3$CN/5% H$_2$O	−1.60	6.6	0.18	[28]
	CH$_3$CN/50% CH$_3$OH	−1.60	22	1.08	
[Cp*Ir(**N2**)Cl]$^+$	CH$_3$CN/50% CH$_3$OH	−1.60	13	0.84	
[Cp*Ir(4DHBP)(OH$_2$)]$^{2+}$	KHCO$_3$ aq.	−0.49[b]	21	4.80	[29]
[Cp*Ir(6DHBP)(OH$_2$)]$^{2+}$	KHCO$_3$ aq.	−0.49[b]	52	4.80	
[(Cp*IrCl)$_2$(THBPM)]$^{2+}$	KHCO$_3$ aq.	−0.49[b]	62	5.00	
[Cp*Ir(**N3**)(OH$_2$)]$^{2+}$	KHCO$_3$ aq.	−0.49[b]	89	5.20	
[Cp*Ir(**N4**)(OH$_2$)]$^+$	KHCO$_3$ aq.	−0.49[b]	95	7.20	
[Fe$_4$N(CO)$_{12}$]$^-$	H$_2$O	−0.96[c]	96	3.80	[30]

[a] E_{app} Applied potential
[b] pH 8.3
[c] pH 7.0

substituent effects on the 2, 4, and 4′ positions of the bipyridine ligand was examined, as outlined in Table 4. More specifically, in CH$_3$CN/5% H$_2$O at −1.60 V, [Cp*Ir(**N1**) Cl]$^+$ bearing an *ortho*-NH$_2$ group (N1, 6-amino-2,2′-bipyridine) produced HCO_2^- with an FE(HCO_2^-) of 6.6% (0.18 mA cm^{-2}). In the case of the [Cp*Ir(**N1**)Cl]$^+$ system, the electrolyte significantly affected the catalytic performance and improved the FE(HCO_2^-) (i.e., to 21.9%) and the current density (i.e., to 1.08 mA cm^{-2}) when CH$_3$CN/50% CH$_3$OH was employed. Interestingly, in CH$_3$CN + 50% CH$_3$OH, formaldehyde (HCHO) was also detected (FE(HCHO) 20.2%), and the selectivity toward HCHO was increased in the case of [Cp*Ir(**N2**)Cl]$^+$ bearing CH$_3$ and CO$_2$Et groups (N2, 4-ethoxycarbonyl-6′-methyl-2,2′-bipyridine; FE(HCHO) 32.2%). Furthermore, cyclic voltammetry studies gave information regarding the reaction mechanism (Scheme 4). Following an initial two-electron reduction of **a**, the resulting iridium(I) species (**b**) was protonated to form iridium(III) hydride (**c**). Subsequently, **c** underwent a bipyridine-centered one-electron reduction prior to transfer of the hydride from **d** to CO$_2$. The dissociation of HCO_2^- from **e** required a further one-electron reduction. An analogous mechanism was also proposed by Meyer and coworkers, which involves the use of a Ru-bipyridine complex in the electrocatalytic reduction of CO$_2$ [27].

Furthermore, [Cp*Ir(4DHBP)(OH$_2$)]$^{2+}$ and [Cp*Ir(6DHBP)(OH$_2$)]$^{2+}$ bearing *ortho*- and *para*-OH groups on the bpy ligand were reported to enable the electrochemical conversion of CO$_2$ to HCO_2^- under a low overpotential and without the requirement for organic solvents (FE(HCO_2^-) 21.0 and 52.0%) [29]. In addition, the current density and FE$_{HCO2-}$ of [(Cp*IrCl)$_2$(THBPM)]$^{2+}$, whereby four OH groups were present on the ligand, were enhanced upon the introduction of OH groups. Furthermore, when one side of the bpy structure was replaced by an imidazoline ([Cp*Ir(**N3**)(OH$_2$)]$^{2+}$) or amide species ([Cp*Ir(**N4**)(OH$_2$)]$^+$), the catalytic activity
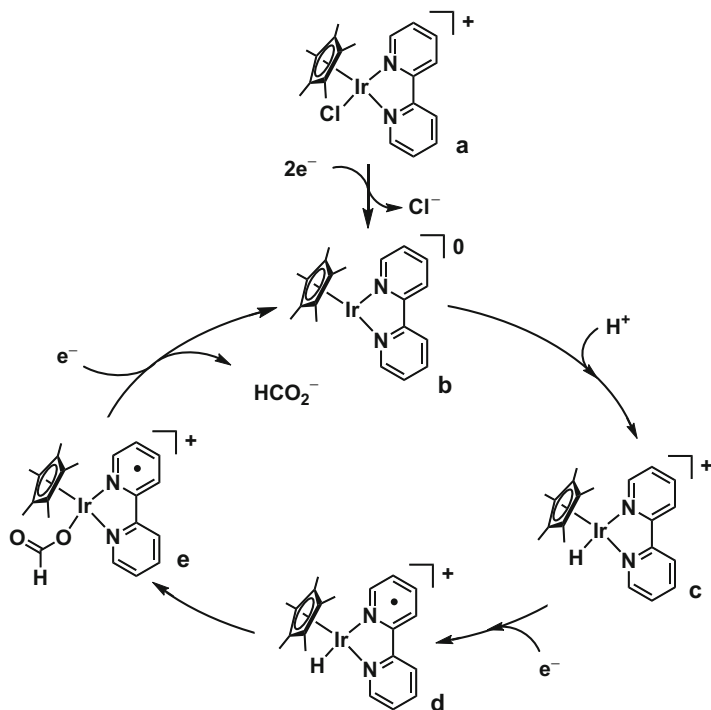
Scheme 4 Proposed mechanism for the electroreduction of CO_2, as proposed by Tzschucke and coworkers

was further enhanced. When the catalytic performances of $[Cp^*Ir(4DHBP)(OH_2)]^{2+}$, $[Cp^*Ir(6DHBP)(OH_2)]^{2+}$, $[(Cp^*IrCl)_2(THBPM)]^{2+}$, $[Cp^*Ir(N3)(OH_2)]^{2+}$, and $[Cp^*Ir(N4)(OH_2)]^+$ were compared, the results were consistent with the order of activity for the hydrogenation of CO_2 [31], thereby indicating that common active species are involved in the electroreduction and hydrogenation of CO_2. Interestingly, combination of the iridium catalyst with different electrode materials indicated that electrodes exhibiting lower hydrogen overpotentials (i.e., a Pt black electrode) led to a remarkable decrease in the applied potential. As a result, the combination of $[Cp^*Ir(N4)(OH_2)]^+$ and a Pt black working electrode gave a high current density (7.20 mA cm^{-2}) and a high FE(HCO_2^-) (95.0%). In addition, electrochemical measurements, electrokinetic analyses, and reaction mechanism studies revealed that the iridium-hydride species detected by ^1H NMR were generated via a two-electron reduction process. The above values represent the lowest overpotential and the highest current density among the previous reports using homogeneous catalysts for the electroreduction of CO_2 to HCO_2^-, and the overpotential was lower than that of the heterogeneous catalyst, thereby indicating that iridium-hydride species are key to the electroreduction of CO_2. A reaction mechanism was proposed in the case of $[Cp^*Ir(N4)(OH_2)]^+$ as follows, whereby $[Cp^*Ir^I(N4)]^-$ was initially
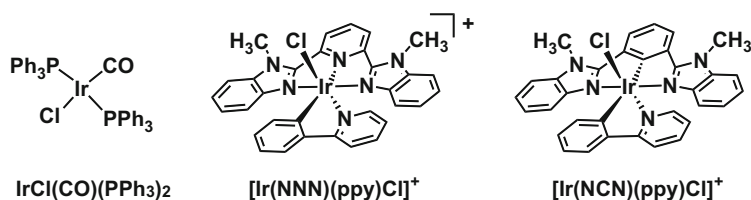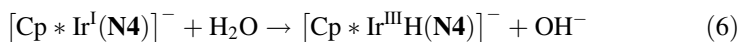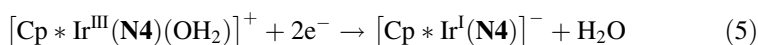
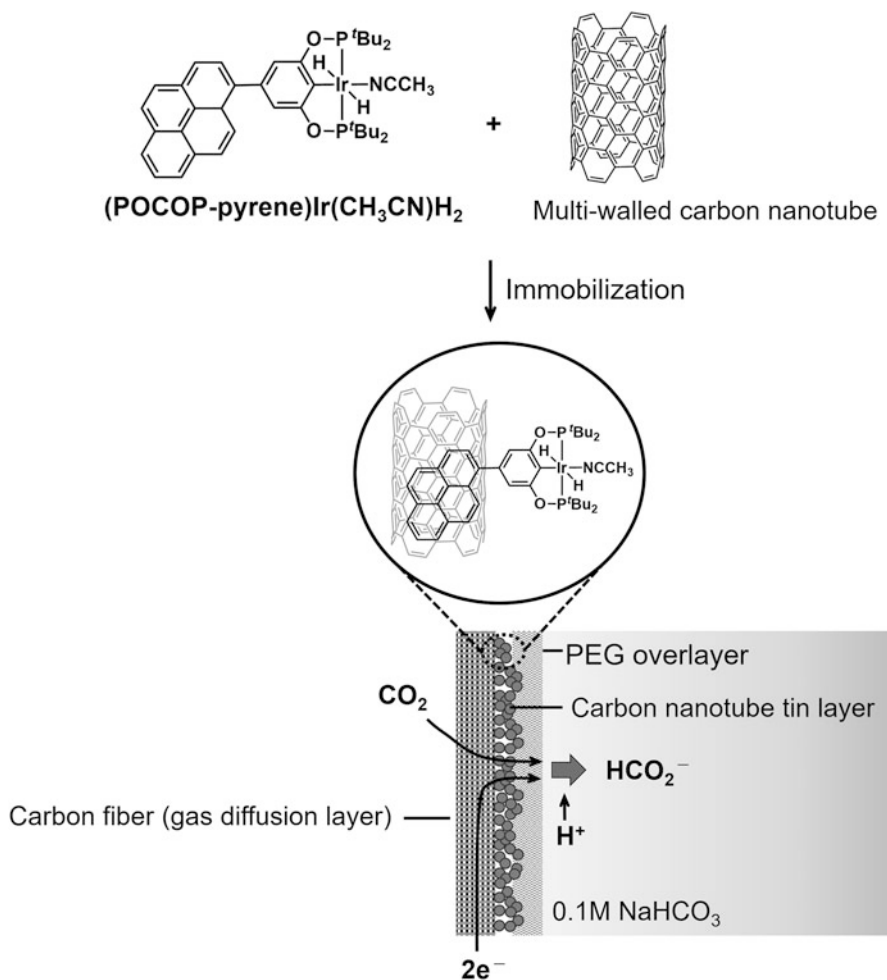**Chart 4** Catalysts for electroreduction of CO_2 to CO

generated by the two-electron reduction of $[Cp*Ir^{III}(\mathbf{N4})(OH_2)]^+$ (Eq. 5). Subsequently, $[Cp*Ir^{III}H(\mathbf{N4})]^+$ produced by the reaction of $[Cp*Ir^{I}(\mathbf{N4})]^-$ with H_2O (Eq. 6) reduced CO_2 to HCO_2^- (Eq. 7). The cathodic current observed under CO_2 was derived so that $[Cp*Ir^{III}(\mathbf{N4})]^+$ was regenerated by the reaction of $[Cp*Ir^{III}H(\mathbf{N4})]^+$ with CO_2.

$$\left[Cp*Ir^{III}(\mathbf{N4})(OH_2)\right]^+ + 2e^- \rightarrow \left[Cp*Ir^{I}(\mathbf{N4})\right]^- + H_2O \tag{5}$$

$$\left[Cp*Ir^{I}(\mathbf{N4})\right]^- + H_2O \rightarrow \left[Cp*Ir^{III}H(\mathbf{N4})\right]^- + OH^- \tag{6}$$

$$\left[Cp*Ir^{III}H(\mathbf{N4})\right]^- + CO_2 + H_2O \rightarrow \left[Cp*Ir^{III}(\mathbf{N4})(OH_2)\right]^+ + HCO_2^- \tag{7}$$

Although the $[Fe_4N(CO)_{12}]^-$ catalyst has been reported to exhibit activity in aqueous solution (Chart 4) [30], the Ir catalyst (i.e., $[Cp*Ir(\mathbf{N4})(OH_2)]^+$) is superior in terms of the overpotential and current density.

2.2 Immobilized Catalysts

Since electron transfer in electrochemical reactions is limited to the very vicinity of the electrode, the reaction is dominated by the diffusion of the catalyst to the electrode in the bulk electrolyte. Therefore, a method of immobilizing the catalyst to the electrode to eliminate the diffusion factor has been attempted [32]. More specifically, an iridium dihydride catalyst bearing a POCOP pincer ligand containing pyrene was immobilized on carbon nanotube-coated gas diffusion electrodes. Compared to (POCOP)IrH$_2$ (1.07 mA cm^{-2}, -1.45 V), (POCOP-pyrene)Ir(CH$_3$CN)H$_2$ exhibited and improved for the electroreduction by immobilization on the electrode in 0.5 M LiClO$_4$, 0.1 M NaHCO$_3$, and 1%v/vCH$_3$CN (3.60 mA cm^{-2}, -1.40 V). Furthermore, through optimization of the reaction system, the gas diffusion electrode interfaced both the gaseous and aqueous phases, significantly enhancing the current densities up to ~15.0 mA cm^{-2}, whereby a high FE$_{HCO2^-}$ was also maintained (Scheme 5). When the gas diffusion electrode interfaced both the gaseous and aqueous phases, (POCOP-pyrene)Ir(CH$_3$CN)H$_2$ was able to access sufficient CO_2 from the gas phase and readily release HCO_2^- into the aqueous phase, thereby

Scheme 5 Illustration of a carbon nanotube-coated gas diffusion electrode with a surface-bound (POCOP-pyrene)Ir(CH$_3$CN)H$_2$ catalyst for the electroreduction of CO$_2$ to HCO$_2^-$

relieving mass transport constraints. The proposed reaction mechanism was comparable to that presented in Scheme 1a.

3 Electroreduction of Carbon Dioxide to Carbon Monoxide

CO is another two-electron reduction product from CO$_2$ and is an important material in C1 chemistry. For example, a mixture of H$_2$ and CO, known as synthesis gas, can be used as a precursor for the production of methanol (CH$_3$OH) and hydrocarbons.

Table 5 Electroreduction of CO_2 to CO

Catalyst	Solvent	E_{app}[a] [V]	FE(CO) [%]	j [mA cm^{-2}]	Ref.
IrCl(CO)(PPh$_3$)$_2$	DMF	−1.31	58	0.16	[33]
	DMF/10% H$_2$O	−1.06	32	0.50	
[Ir(NNN)(ppy)Cl]$^+$	CH$_3$CN	−1.13	>99	–	[34]
[Ir(NCN)(ppy)Cl]	CH$_3$CN	−1.67	45 ± 5	–	

[a]E_{app} Applied potential

In general, since the reduction of CO_2 and H^+ on the cathode competes during the electroreduction of CO_2, the suppression of H_2 generation is necessary to improve the selectivity. On the other hand, from the viewpoint of synthesis gas production, H_2 generation is not a disadvantage; if the H_2/CO ratios can be controlled with a catalyst, not only CO but also synthesis gas can be produced directly. However, the reduction of CO_2 to CO requires a large amount of energy, and even in the presence of strong reducing agents, overcoming the O=CO bond enthalpy of 532 kJ mol^{-1} often presents kinetic difficulties.

The first electroreduction of CO_2 to CO using a homogeneous iridium catalyst (Chart 4, Table 5), reported by Pruchnik and coworkers [33], involved the reaction of IrCl(CO)(PPh$_3$)$_2$ in DMF or DMF + 10% H_2O. Using DMF, CO production at −1.31 V was observed with an FE(CO) of 58% (0.16 mA cm^{-2}). In addition, formic acid was found in the electrolyte. When 10% H_2O was added, although the current density increased to 0.5 mA cm^{-2}, the FE(CO) was 32%. In this case, along with CO and formic acid, a trace of H_2 was detected. They also proposed a mechanism for the reaction between the iridium-hydride intermediates and CO_2; however, spectroscopic data were not reported.

Fujita and coworkers described the electroreduction process and density functional theory (DFT) calculations using [Ir(NNN)(ppy)Cl]$^+$ and [Ir(NCN)(ppy)Cl]$^+$ (ppy, 2-phenylpyridine) [34]. When using [Ir(NNN)(ppy)Cl]$^+$, selective CO formation was achieved at −1.13 V (FE(CO) > 99%), while [Ir(NCN)(ppy)Cl] yielded CO with an FE(CO) of 45 ± 5% and HCO_2^- with an FE(HCO_2^-) of 5–10%. In both cases, H_2 production was not detected. The production of HCO_2^- is supported by the DFT calculations that show iridium-hydride intermediates exhibiting a high hydricity and where CO_2 insertion is thermodynamically favorable. Interestingly, the ligand exchange from Cl^- to CH_3CN, [Ir(NNN)(ppy)(NCCH$_3$)]$^{2+}$, functions as a photocatalyst and can convert CO_2 to CO.

However, the mechanism for CO production using iridium catalysts was not clear, despite reaction mechanisms being reported for other metal complexes. For example, using a Pd complex bearing a pincer ligand, cyclic voltammetry and potentiostatic electrolysis measurements revealed that Pd-CO_2^- species with η^1-C coordination were generated via an electrochemical one-electron reduction process, and Pd-COOH intermediates were produced by the reduction and protonation of these Pd-CO_2^- species. Furthermore, the intermediates were protonated to generate a Pd-CO species, and finally CO was eliminated to regenerate the active species [35].

4 Electroreduction of Carbon Dioxide to Oxalate

C-C bond formation is an important reaction in chemical synthesis that is commonly carried out through coupling reactions with organometallic reagents. In this context, the use of $C_2O_4^{2-}$ as a C2 compound is interesting from the viewpoint of electrochemical C-C bond formation. In addition, $C_2O_4^{2-}$ are useful chemicals; for example, dimethyl $C_2O_4^{2-}$ is a precursor for the production of ethylene glycol and methyl glycolate [36].

When the electroreduction of CO_2 was conducted in CH_3CN at -1.40 V, trinuclear iridium complex $[(Cp^*Ir)_3(\mu_3\text{-}S)_2]^{2+}$ gave $C_2O_4^{2-}$ ($FE(C_2O_4^{2-})$ 64%) and $[(Cp^*Ir)_2(Ir(\eta^4\text{-}C_5(CH_3)_5)CH_2CN)(\mu_3\text{-}S)_2]^+$ ($[(Cp^*Ir)_3CH_2CN(\mu_3\text{-}S)_2]^+$) [37]. The crystal structure of $[(Cp^*Ir)_3CH_2CN(\mu_3\text{-}S)_2]^+$ was determined by X-ray diffraction, and it was found that a linear CH_2CN group was linked at the exo-position of a Cp* ligand, and the $C_5(CH_3)_5CH_2CN$ ligand was coordinated to an iridium atom in the η^4-mode. In addition, the cyclic voltammogram of $[(Cp^*Ir)_3CH_2CN(\mu_3\text{-}S)_2]^+$ recorded in CH_3CN in the presence of CO_2 exhibited a strong catalytic current due to the reduction of CO_2, although this was not observed for $[(Cp^*Ir)_3(\mu_3\text{-}S)_2]^{2+}$. As shown in Scheme 6, the reduced form of $[(Cp^*Ir)_3CH_2CN(\mu_3\text{-}S)_2]^+$ works as the active species in the reduction of CO_2. The direct attack of CO_2 on the Ir species of $[(Cp^*Ir)_3CH_2CN(\mu_3\text{-}S)_2]^+$ is blocked by the Cp^*, $(\eta^4\text{-}C_5(CH_3)_5)CH_2CN$, and μ_3-S ligands, while there seems to be no serious
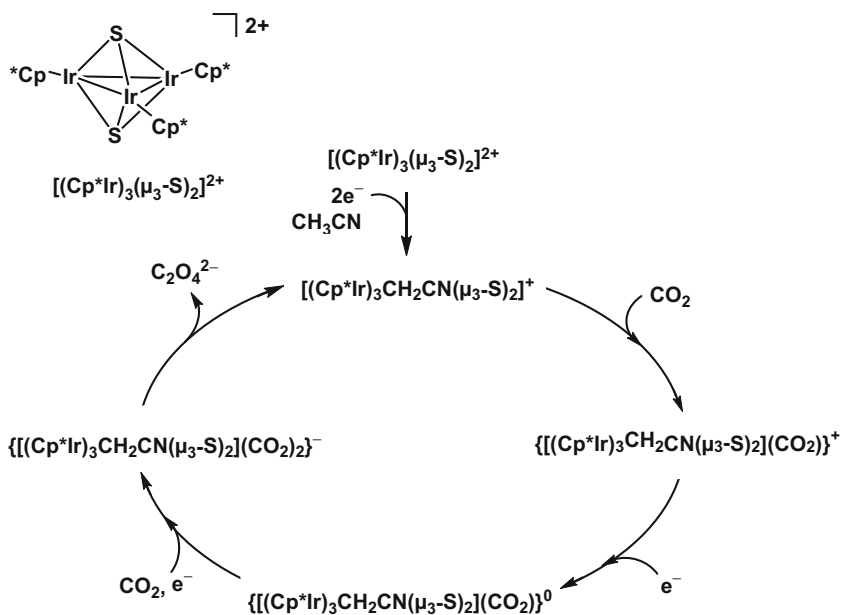
Scheme 6 Proposed mechanism for electroreduction of CO_2 to $C_2O_4^{2-}$ using $[(Cp^*Ir)_3(\mu_3\text{-}S)_2]^{2+}$

steric hindrance for an electrophilic attack of CO_2 to the μ_3-S ligand $(\{[(Cp^*Ir)_3CH_2CN(\mu_3\text{-}S)_2](CO_2)\}^+)$. In addition, a two-electron reduction and subsequent reaction with CO_2 provided anionic species $\{[(Cp^*Ir)_3CH_2CN(\mu_3\text{-}S)_2](CO_2)_2\}^-$. The coupling of two CO_2 molecules bonded on adjacent μ_3-S and Ir centers in $\{[(Cp^*Ir)_3CH_2CN(\mu_3\text{-}S)_2](CO_2)_2\}^-$ produced $C_2O_4{}^{2-}$. It should also be noted that the electrochemical conversion of CO_2 to $C_2O_4{}^{2-}$ has been achieved using Fe [38], Ni [39, 40], Cu [41], and Ru complexes [42], in addition to $[(Cp^*Ir)_3(\mu_3\text{-}S)_2]^{2+}$.

5 Conclusion

The development of iridium-based catalysts for the electrolytic reduction of CO_2 has been conducted for more than 30 years. Due to the increasing importance of CO_2 utilization technologies in recent years, selective CO_2 conversion has become possible, with dramatically improved catalyst performances being obtained through the development of new ligands. In addition, the overpotential and current density for the electroreduction of CO_2 have also received attention in terms of the energy consumption and reaction rate. In terms of the overpotential, it is important to understand the function of metal-hydride species, as discussed in this chapter. Furthermore, it has been found that the reaction system, and more specifically the electrode materials and mass diffusion, has a significant effect on the reaction efficiency. Hence, to achieve efficient reactions with high current densities and low overpotentials, the design of an appropriate catalyst and overall electrochemical system must be optimized.

In the context of future catalyst developments, compounds that require C-O bond cleavage and multiple C-H bond formation, such as CH_3OH, will be targeted. Indeed, the catalytic functions of single C-H bond formation and C-O bond cleavage, such as in the cases of $HCO_2{}^-$ formation and CO formation, have been studied. In terms of the synthesis of CH_3OH, the integration of individual catalyst design principals will be necessary.

References

 1. Rogelj J, den Elzen M, Höhne N, Fransen T, Fekete H, Winkler H, Schaeffer R, Sha F, Riahi K, Meinshausen M (2016) Nature 534:631–639
 2. Ilas A, Ralon P, Rodriguez A, Taylor M (2018) International Renewable Energy Agency (IRENA). Abu Dhabi, UAE, pp 1–160
 3. Gotz M, Lefebvre J, Mors F, Koch AM, Graf F, Bajohr S, Reimert R, Kolb T (2016) Renew Energy 85:1371–1390
 4. Schemme S, Samsun RC, Peters R, Stolten D (2017) Fuel 205:198–221
 5. Whipple DT, Kenis PJA (2010) J Phys Chem Lett 1:3451–3458
 6. Benson EE, Kubiak CP, Sathrum AJ, Smieja JM (2009) Chem Soc Rev 38:89–99

7. Taheri A, Berben LA (2016) Chem Commun 52:1768–1777
8. Qiao J, Liu Y, Hong F, Zhang J (2014) Chem Soc Rev 43:631–675
9. Fujita E, Brunschwig BS (2001) Catalysis of electron transfer, heterogeneous systems, gas phase systems. In: Balzani V (ed) Electron transfer in chemistry, vol 1. Wiley, Weinheim, pp 88–126
10. Zhang L, Zhao Z-J, Gong J (2017) Angew Chem Int Ed 56:11326–11353
11. Francke R, Schille B, Roemelt M (2018) Chem Rev 118:4631–4701
12. Zhang S, Fan Q, Xia R, Meyer TJ (2020) Acc Chem Res 53:255–264
13. Wang W-H, Himeda Y, Muckerman JT, Manbeck GF, Fujita E (2015) Chem Rev 115:12936–12973
14. Boddien A, Gärtner F, Federsel C, Sponholz P, Mellmann D, Jackstell R, Junge H, Beller M (2011) Angew Chem Int Ed 50:6411–6414
15. Kawanami H, Iguchi M, Himeda Y (2020) Inorg Chem 59:4191–4199
16. Cheng SC, Blaine CA, Hill MG, Mann KR (1996) Inorg Chem 35:7704–7708
17. Caix C, ChardonNoblat S, Deronzier A (1997) J Electroanal Chem 434:163–170
18. Tanaka R, Yamashita M, Nozaki K (2009) J Am Chem Soc 131:14168–14169
19. Schmeier TJ, Dobereiner GE, Crabtree RH, Hazari N (2011) J Am Chem Soc 133:9274–9277
20. Kang P, Cheng C, Chen Z, Schauer CK, Meyer TJ, Brookhart M (2012) J Am Chem Soc 134:5500–5503
21. Kang P, Meyer TJ, Brookhart M (2013) Chem Sci 4:3497–3502
22. Ahn ST, Bielinski EA, Lane EM, Chen Y, Bernskoetter WH, Hazari N, Palmore GTR (2015) Chem Commun 51:5947–5950
23. Bi J, Hou P, Kang P (2019) ChemCatChem 11:2069–2072
24. Cao L, Sun C, Sun N, Meng L, Chen D (2013) Dalton Trans 42:5755–5763
25. Osadchuk I, Tamm T, Ahlquist MSG (2016) ACS Catal 6:3834–3839
26. Cunningham DW, Barlow JM, Velazquez RS, Yang JY (2020) Angew Chem Int Ed 59:4443–4447
27. Pugh JR, Bruce MRM, Sullivan BP, Meyer TJ (1991) Inorg Chem 30:86–91
28. Sypaseuth FD, Matlachowski C, Weber M, Schwalbe M, Tzschucke CC (2015) Chem Eur J 21:6564–6571
29. Kanega R, Onishi N, Wang L, Himeda Y (2018) ACS Catal 8:11296–11301
30. Taheri A, Thompson EJ, Fettinger JC, Berben LA (2015) ACS Catal 5:7140–7151
31. Kanega R, Onishi N, Szalda DJ, Ertem MZ, Muckerman JT, Fujita E, Himeda Y (2017) ACS Catal 7:6426–6429
32. Kang P, Zhang S, Meyer TJ, Brookhart M (2014) Angew Chem Int Ed 53:8709–8713
33. Szymaszek A, Pruchnik FP (1989) J Organomet Chem 376:133–140
34. Manbeck GF, Garg K, Shimoda T, Szalda DJ, Ertem MZ, Muckerman JT, Fujita E (2017) Faraday Discuss 198:301–317
35. Rakowski Dubois M, Dubois DL (2009) Acc Chem Res 42:1974–1982
36. Yue H, Zhao Y, Ma X, Gong J (2012) Chem Soc Rev 41:4218–4244
37. Tanaka K, Kushi Y, Tsuge K, Toyohara K, Nishioka T, Isobe K (1998) Inorg Chem 37:120–126
38. Pun S-N, Chung W-H, Lam K-M, Guo P, Chan P-H, Wong K-Y, Che C-M, Chen T-Y, Peng S-M (2002) J Chem Soc Dalton Trans:575–583
39. Rudolph M, Dautz S, Jäger E-G (2000) J Am Chem Soc 122:10821–10830
40. Udugala-Ganehenege MY, Dissanayake NM, Liu Y, Bond AM, Zhang J (2014) Transit Met Chem 39:819–830
41. Angamuthu R, Byers P, Lutz M, Spek AL, Bouwman E (2010) Science 327:313–315
42. Ali MM, Sato H, Mizukawa T, Tsuge K, Haga M, Tanaka K (1998) Chem Commun:249–250